Neuro-Oncology

Neuro-Oncology 16(5), 662–670, 2014
doi:10.1093/neuonc/not235
Advance Access date 18 December 2013

Contrast enhancement in 1p/19q-codeleted anaplastic oligodendrogliomas is associated with 9p loss, genomic instability, and angiogenic gene expression

German Reyes-Botero, Caroline Dehais, Ahmed Idbaih, Nadine Martin-Duverneuil, Marion Lahutte, Catherine Carpentier, Eric Letouzé, Olivier Chinot, Hugues Loiseau, Jerome Honnorat, Carole Ramirez, Elisabeth Moyal, Dominique Figarella-Branger, François Ducray, and POLA Network†

AP-HP, Groupe Hospitalier Pitié-Salpêtrière, Paris, France (G.R.B., C.D., A.I.); Université Pierre et Marie Curie–Paris 6, Centre de Recherche de l'Institut du Cerveau et de la Moelle Epinière, Paris, France (A.I., C.C.); AP-HP, Groupe Hospitalier Pitié-Salpêtrière, Service de Neuro-radiologie, Paris, France (N.M.-D.); Service de Santé des Armées, Hôpital d'Instruction des Armées, Paris, France (M.L.); Programme Carte d'Identité des Tumeurs, Ligue Nationale Contre le Cancer, Paris, France (E.L.); AP-HM, Hôpital de la Timone, Service de Neuro-Oncologie, Marseille , France (O.C.); CHU Bordeaux, Hôpital Pellegrin, Service de Neurochirurgie, Bordeaux, France (H.L.); Hospices Civils de Lyon, Hôpital Pierre Wertheimer, Service de Neuro-Oncologie, Bron, France (J.H., F.D.); INSERM U1028, CNRS UMR5292, Bron, France (J.H., F.D.); CHU Lille, Hôpital Roger Salengro, Clinique de Neurochirurgie, Lille, France (C.R.); Institut Claudius Regaud, Département de Radiothérapie, Toulouse, France (E.M.); AP-HM, Hôpital de la Timone, Service d'Anatomie Pathologique et de Neuropathologie, Marseille, France (D.F.-B.); Université de la Méditerranée, Aix-Marseille, Faculté de Médecine La Timone, Marseille, France (D.F.B.)

Corresponding author: Caroline Dehais, MD, Service de Neurologie 2-Mazarin, Groupe Hospitalier Pitié-Salpêtrière. 47-83, Boulevard de l'Hôpital, 75013 Paris, France (caroline.dehais@psl.aphp.fr).

†**POLA network:** Amiens: Christine Desenclos, Henri Sevestre; Angers: Philippe Menei, Sophie Michalak, Edmond Al Nader; Besançon: Joel Godard, Gabriel Viennet; Bobigny: Antoine Carpentier; Bordeaux: Sandrine Eimer; Brest :Phong Dam-Hieu, Isabelle Quintin-Roué; Caen: Jean-Sebastien Guillamo, Emmanuelle Lechapt-Zalcman; Clermont-Ferrand: Jean-Louis Kemeny, Pierre Verrelle; Clichy: Thierry Faillot; Colmar: Claude Gaultier, Marie Christine Tortel; Créteil: Christo Christov, Caroline Le Guerinel; Dijon: Marie-Hélène Aubriot-Lorton, Francois Ghiringhelli; Grenoble: François Berger; Kremlin-Bicêtre: Catherine Lacroix, Fabrice Parker; Lille: François Dubois, Claude-Alain Maurage; Limoges: Edouard-Marcel Gueye, Francois Labrousse; Lyon: Anne Jouvet; Montpellier: Luc Bauchet, Valérie Rigau; Nancy: Patrick Beauchesne, Jean-Michel Vignaud; Nantes: Mario Campone, Delphine Loussouarn; Nice: Denys Fontaine, Fanny Vandenbos; Nîmes: Chantal Campello, Pascal Roger; Orleans: Melanie Fesneau, Anne Heitzmann; Paris: Jean-Yves Delattre (coordinator), Selma Elouadhani, Karima Mokhtari, Marc Polivka, Damien Ricard; Poitiers: Pierre-Marie Levillain, Michel Wager; Reims: Philippe Colin, Marie-Danièle Diebold; Rennes: Dan Chiforeanu, Elodie Vauleon; Rouen: Olivier Langlois, Annie Laquerriere; Saint-Etienne: Marie Janette Motsuo Fotso, Michel Peoc'h; Saint Pierre de la Réunion: Marie Andraud, Servane Mouton; Strasbourg: Marie-Pierre Chenard, Georges Noel; Toulon: Nicolas Desse, Raoulin Soulard; Toulouse: Alexandra Amiel-Benouaich, Emmanuelle Uro-Coste; Villejuif: Frederic Dhermain.

Background. The aim of this study was to correlate MRI features and molecular characteristics in anaplastic oligodendrogliomas (AOs).

Methods. The MRI characteristics of 50 AO patients enrolled in the French national network for high-grade oligodendroglial tumors were analyzed. The genomic profiles and *IDH* mutational statuses were assessed using high-resolution single-nucleotide polymorphism arrays and direct sequencing, respectively. The gene expression profiles of 25 1p/19q-codeleted AOs were studied on Affymetrix expression arrays.

Results. Most of the cases were frontal lobe contrast-enhanced tumors (52%), but the radiological presentations of these cases were heterogeneous, ranging from low-grade glioma-like aspects (26%) to glioblastoma-like aspects (22%). The 1p/19q codeletion ($n = 39$) was associated with locations in the frontal lobe ($P = .001$), with heterogeneous intratumoral signal intensities ($P = .003$) and with no or nonmeasurable contrast enhancements ($P = .01$). The *IDH* wild-type AOs ($n = 7$) more frequently displayed ringlike contrast enhancements ($P = .03$) and were more frequently located outside of the frontal lobe ($P = .01$). However, no specific imaging pattern could be identified for the 1p/19q-codeleted AO or the *IDH*-mutated AO. Within the 1p/19q-codeleted AO, the contrast enhancement was associated with larger tumor volumes ($P = .001$), chromosome 9p loss and *CDKN2A* loss ($P = .006$), genomic instability ($P = .03$), and angiogenesis-related gene expression ($P < .001$), particularly for vascular endothelial growth factor A and angiopoietin 2.

Conclusion. In AOs, the 1p/19q codeletion and the *IDH* mutation are associated with preferential (but not with specific) imaging characteristics. Within 1p/19q-codeleted AO, imaging heterogeneity is related to additional molecular alterations, especially chromosome 9p loss, which is associated with contrast enhancement and larger tumor volume.

Received 25 July 2013; accepted 8 November 2013

Keywords: anaplastic oligodendroglioma, *IDH* mutation, magnetic resonance imaging, SNP array, 1p19q co-deletion.

Anaplastic oligodendrogliomas (AOs) account for approximately 10% of gliomas.[1] Despite the homogeneous histological appearances of the AOs, the survival times of AO patients range from a few years to more than 15 years. This clinical heterogeneity has been related to molecular heterogeneity.[2,3] Three main molecular subgroups of AO can be distinguished.[4] Anaplastic oligodendrogliomas with 1p/19q codeletion (virtually all mutated by the isocitrate dehydrogenase [IDH] gene) display the best prognosis. The *IDH*-mutated AOs, without 1p/19q codeletions, have an intermediate prognosis. Finally, non-1p/19q-codeleted and non-*IDH*-mutated AOs have a poor prognosis. In addition to the clinical and molecular heterogeneities, the radiological presentations of AO also vary. In AO, the 1p/19q codeletion has been shown to be associated with distinct radiological characteristics, particularly frontal lobe location, blurred tumor borders, and intratumoral signal heterogeneity.[5–9] In glioblastomas, several studies have correlated imaging, genomic, and gene expression features. These studies identified gene expression modules associated with contrast enhancement, edema, and necrosis and showed that *IDH* mutation, amplification of the epidermal growth factor receptor gene (*EGFR*), and glioblastoma transcriptomic subgroups were associated with preferential radiological features.[10–13] The aims of the present study were to describe the radiological characteristics of 50 AO patients enrolled in the French network for AO and to correlate these characteristics with tumor molecular profiles (ie, copy number and gene expression profiles) and *IDH* mutational status.

Materials and Methods

The POLA Network

The scarcity of AO requires collaborative multicenter networks to investigate large cohorts of AO patients. To improve the clinical, biological, and translational research focused on AO patients, in 2009 the French Institut National du Cancer supported the creation of a national network named "Prise en charge des OLigodendrogliomes Anaplasiques" (POLA). This network prospectively collects samples and data from patients with a diagnosis of high-grade oligodendroglial tumor made in the main academic centers of the country.[14]

Patients

Fifty newly diagnosed AO patients in the POLA network for whom initial MRI results were available have been included in this study. The diagnosis of AO was confirmed by a central pathological review (D.F-B., A.J., K.M., E.U.C.) using criteria from the World Health Organization.[15] All of the patients provided written consent for the clinical data collection and the genetic analysis, according to national and POLA policies.

Radiological Study

Two neuroradiologists (N.M.D., M.L.) and 2 neurologists (G.R.B., C.D.), all of whom were blinded to molecular status, retrospectively analyzed the preoperative conventional brain MRIs (1.5 or 3 T). All MRIs were obtained within 4 weeks of the histological diagnosis (biopsy or surgery) and included the following images: T1-weighted, T1-weighted postgadolinium, and T2-weighted or T2 fluid attenuated inversion recovery (FLAIR). The following characteristics were assessed (Fig. 1): (i) tumor location (frontal, temporal, insula, parietal, occipital, basal ganglia, corpus callosum); (ii) unilobar or multilobar involvement; (iii) contrast enhancement as absent, blurry (nonmeasurable), or measurable (nodular or ringlike); (iv) shape of the tumor borders (sharp, blurred) on T2/FLAIR sequences; (v) signal intensity (homogeneous vs heterogeneous), where heterogeneous intratumoral signal intensity was defined as the coexistence of hyposignal and hypersignal zones; (vi) intratumoral cysts ($>$1 cm); and (vii) tumor volume, as calculated by manual segmentation (OsiriX v3.8.1 32-bit software).

DNA and RNA Extraction

The iPrep ChargeSwitch Forensic Kit was used to extract DNA from frozen tumor samples, and the RNeasy Lipid Tissue Mini Kit (Qiagen) was used to extract total RNA. Both the RNA and the DNA were assessed for integrity and quantity, following stringent quality control criteria established by the program protocols of the Cartes d'Identité des Tumeurs (http://cit.ligue-cancer.net). A 1-μg volume from each DNA sample was outsourced to the Integragen Company (Paris, France) for single-nucleotide polymorphism (SNP) array experiments.[14] A 1-μg volume from each RNA sample was used to perform the gene expression analysis.

SNP Array and Gene Expression Array Procedures

As mentioned above, the SNP array experiments were outsourced to Integragen. Two types of platforms were used: HumanCNV370-Quad and Human610-Quad from Illumina.[14] Because the molecular abnormalities were included in the medical management of the patients (ie, non-1p/19q-codeleted patients were included in the European Organisation for Research and Treatment of Cancer 26053-22054 trial if they were eligible), the tumor DNA was run prospectively to obtain its genomic profile within 10 days of the tumor resection. The gene expression profiles of 25 tumors with sufficient RNA available were studied on gene expression arrays. These arrays were performed using the IGBMC (Institut de Génétique et de Biologie Moléculaire et Cellulaire) microarray platform. Total RNA was amplified, labeled, and hybridized to the Affymetrix Human Genome U133 plus2 GeneChip following the manufacturer's protocol. The microarrays were scanned using an Affymetrix GeneChip Scanner 3000, and the raw intensities were quantified from the subsequent images using GCOS 1.4 software (Affymetrix). The data were normalized using the Robust Multi-array Average method implemented in the R package affy.[16]

1p/19q Codeletion

Tumors were considered as codeleted if there was an entire loss of 1p and an entire loss of 19q with centromeric breakpoints.[14]

IDH1 and IDH2 Mutational Status

IDH1 codon 132 and *IDH2* codon 172 were sequenced using the Sanger method with the following primers as previously reported:[17] IDH1 forward: TGTGTTGAGATGGACGCCTATTTG, and IDH1 reverse: TGCCACCAACGACCAAGTC; and IDH2 forward: GCCCGGTCTGCCACAAAGTC, and IDH2 reverse: TTGGCAGACTCCAGAGCCCA.

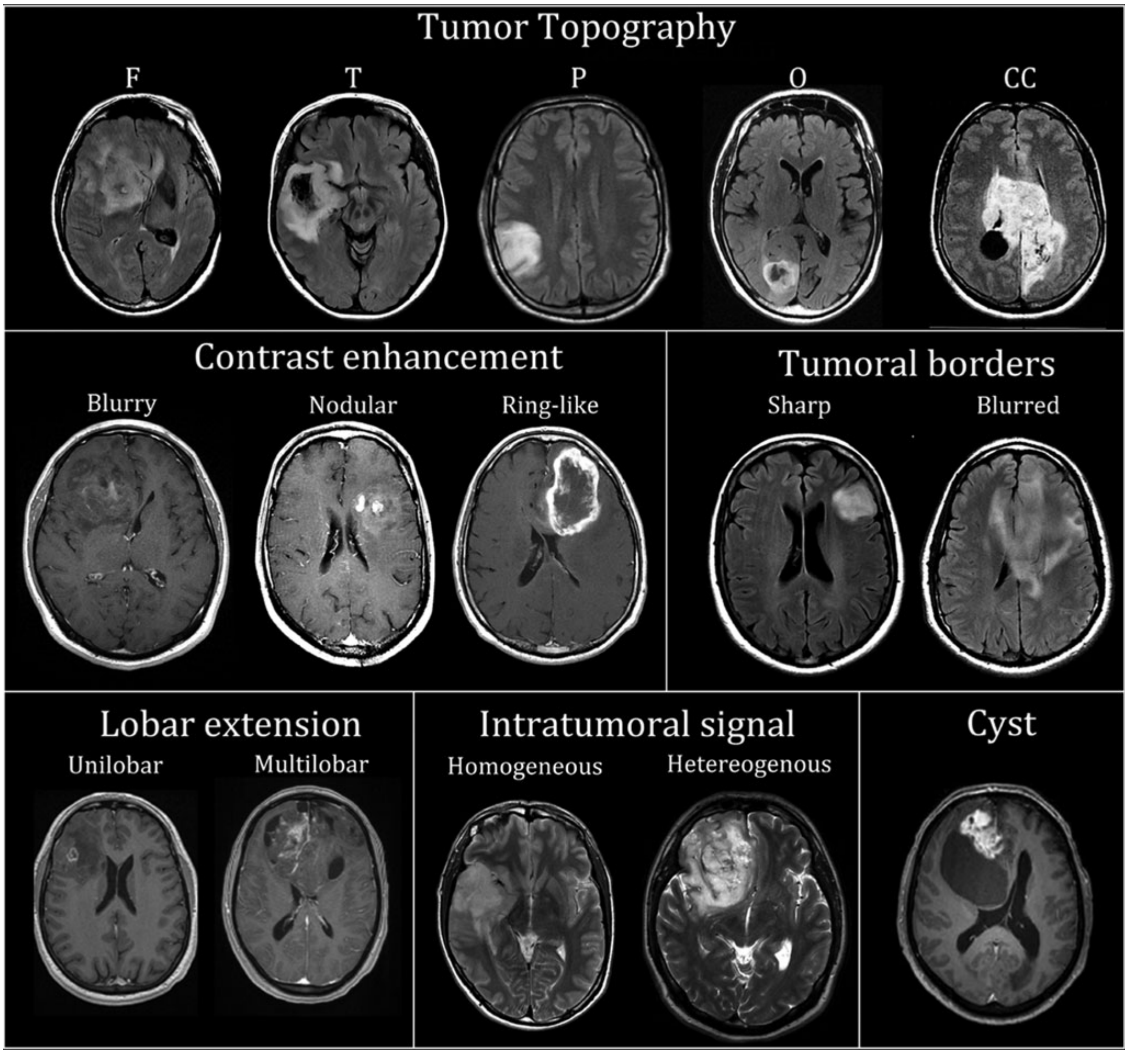

Fig. 1. A representative example of the MRI features assessed in the 50 AOs. Upper panel: tumor topography—F: frontal, T: temporal, P: parietal, O: occipital, CC: corpus callosum. Middle panel: Contrast enhancement types (left), tumor borders in T2/FLAIR sequences (right). Lower panel: Lobar extension—unilobar or multilobar, intratumoral signal, cyst (diameter >1 cm).

Statistical Analyses

The SNP array analysis was performed as previously described.[14] The association of chromosome arm imbalances (either loss or gain) with radiological variables was estimated using either Fisher's exact test (for factors) or Student's *t*-test (for quantitative variables). The gene expression array analysis was performed as previously described.[16] The published centroid-based classifier of Verhaak et al[18] was used to classify our samples according to their system.

Results

Radiological Spectrum of Anaplastic Oligodendrogliomas

The clinical and molecular characteristics of the 50 patients are summarized in Table 1, and their radiological characteristics are summarized in Table 2. Most of the cases were located in the frontal lobe ($n = 35$, 70%), were contrast enhanced ($n = 37$, 74%), and had heterogeneous intratumoral signal intensities ($n = 42$, 84% on T1; $n = 37$, 74% on T2 or FLAIR). However, as shown in Fig. 2, the radiological presentation was highly variable, ranging from a non-contrast-enhanced tumor ($n = 13$, 26%), suggestive of low-grade glioma, to a ringlike enhanced tumor ($n = 11$, 22%), suggestive of glioblastoma.

1p/19q Codeletion and IDH *Mutation Are Associated With Distinct Radiological Features*

Thirty-nine AOs (78%) were 1p/19q codeleted and *IDH* mutated, 4 AOs (8%) were non–1p/19q codeleted and *IDH* mutated, and 7 AOs (14%) had none of these alterations. Their radiological characteristics, categorized by 1p/19q codeletion and *IDH* mutation, are summarized in Table 2 and illustrated in Fig. 2.

The 1p/19q codeletion was associated with a frontal lobe location (32/39 vs 3/11, $P = .001$), heterogeneous intratumoral intensity on T2 or FLAIR (33/39 vs 4/11, $P = .003$), and an absent or nonmeasurable contrast enhancement (21/39 vs. 1/10, $P = .01$).

Table 1. The clinical and relevant molecular characteristics of the 50 patients

Median age (range)	48 y (24–78)
Sex (M/F)	$n=31/n=19$
Symptoms at diagnosis	
Seizures	$n=26$ (52%)
Headache	$n=11$ (22%)
Neurological deficit	$n=13$ (26%)
Cognitive impairment	$n=12$ (24%)
Time from symptom onset to diagnosis	
Median (range)	2.7 mo (0.2–172)
Time from MRI to surgery	
Median (range)	10 d (1–32)
Surgery	
Total resection	$n=13$ (26%)
Subtotal	$n=17$ (34%)
Partial resection	$n=10$ (20%)
Biopsy	$n=10$ (20%)
Molecular alterations	
IDH mutation	$n=43$ (86%)
IDH1	38
IDH2	5
1p/19q codeletion	$n=39$ (78%)
9p loss	$n=16$ (32%)
10q loss	$n=5$ (10%)
EGFR amplification	$n=2$ (4%)

Intratumoral cysts also occurred more frequently in the 1p/19q-codeleted tumors (13/39 vs 1/11, $P=.1$). The *IDH* mutation was also associated with a frontal lobe location (33/43 vs 2/7, $P=.01$; Table 2). The *IDH* wild-type AOs were more frequently parietal (2/7 vs 1/43, $P=.05$) and more frequently displayed ringlike enhancement than *IDH*-mutated AOs (4/7 vs 7/43, $P=.03$).

Although 1p/19q codeletion and *IDH* mutation were associated with distinct radiological features, no radiological pattern was specific to these molecular alterations. As shown in Fig. 2, the radiological presentations of the 1p/19q-codeleted AOs remained variable, ranging from a low-grade-like aspect without contrast enhancement (12/39, 30%) to a glioblastoma-like aspect with ring contrast enhancement (7/39, 18%).

Contrast Enhancement Is Associated With Chromosome 9p Loss in 1p/19q-Codeleted Anaplastic Oligodendrogliomas

To assess whether the radiological heterogeneity within 1p/19q-codeleted AOs was related to their underlying molecular heterogeneity, the genomic profiles of non-contrast-enhanced and contrast-enhanced 1p/19q-codeleted AOs were compared. The contrast-enhanced AOs had a larger mean tumor volume than the non-contrast-enhanced 1p/19q-codeleted AOs (145 vs 61 cm^3, $P=.001$), were more frequently multilobar (13/27 vs 1/12, $P=.02$), and tended to infiltrate the corpus callosum more frequently (11/27 vs 2/12, $P=.2$). In addition, contrast enhancement was associated at the histological level with microvascular proliferation (26/27 vs 6/12, $P=.002$), necrosis (10/27 vs 0/12, $P=.02$), and a higher proliferation index (mean labeling of KI-67 1, 20% vs 15%, $P=.04$).

As shown in Fig. 3, loss of chromosome 9p and the cyclin-dependent kinase inhibitor 2A gene (*CDKN2A*) were more frequent in contrast-enhanced 1p/19q-codeleted AOs compared with non-contrast-enhanced 1p/19q-codeleted AOs (12/27 vs 0/12, respectively, $P=.006$). The contrast-enhanced tumors also exhibited more complex genomic profiles compared with the non-contrast-enhanced tumors. Indeed, the mean number of chromosome alterations and the number of cases displaying more than 3 chromosome arm abnormalities (excluding 1p/19q codeletion) were higher in contrast-enhanced tumors than in non-contrast-enhanced tumors (3.9 vs 1.9, $P=.03$ and 8/27 vs 0/12, $P=.04$, respectively). In addition, there was a positive correlation between the tumor volume and the number of chromosome arm alterations ($r=0.33$, $P=.04$). Consistent with the association between contrast enhancement and tumor volume, chromosome 9p and *CDKN2A* loss in 1p/19q-codeleted AO was also associated with larger tumor volume (median 163 vs 100 cm^3, $P=.02$), multilobar involvement (9/12 vs 5/27, $P=.001$), and corpus callosum infiltration (9/12 vs 4/27, $P=.005$).

Contrast Enhancement Is Associated With the Expression of Angiogenesis-related Genes in 1p/19q-Codeleted Anaplastic Oligodendrogliomas

To identify genes for which expression was associated with contrast enhancement in the 1p/19q-codeleted AOs, the gene expression profiles of contrast-enhanced ($n=18$) and non-contrast-enhanced tumors ($n=7$) were compared using Affymetrix expression arrays. Fifty-nine genes were differentially expressed with a fold change ≥2 and a P value <.005 (Supplementary Table 1). The list of upregulated genes in the contrast-enhanced tumors ($n=33$) was significantly enriched in genes involved in angiogenesis ($P<10^{-4}$), basement membrane ($P<10^{-4}$), and cell adhesion ($P<10^{-4}$). Angiogenesis-related genes consisted of both angiogenic and anti-angiogenic genes (Table 3). In addition, the expression of several angiogenic genes, including angiopoietin 2 (ANGPT2) and vascular endothelial growth factor A (VEGFA), were positively correlated with tumor volume (Table 3). Consistent with VEGFA upregulation, gene set enrichment analysis demonstrated significant enrichments of VEGFA targets ($P<.001$) and hypoxia-related genes ($P<.001$) in the contrast-enhanced tumors (Supplementary Table 2).[19] The contrast-enhanced tumors were also enriched in genes upregulated in glioblastomas compared with low-grade glioma vessels ($P=.02$)[20] and in genes positively correlated with contrast enhancement in glioblastomas ($P=.1$)[11] (Table 3, Supplementary Table 2). Finally, the 25 tumors were classified according to the system of Verhaak et al[18] to assess whether the type of contrast enhancement was associated with AO molecular subclasses. Sixteen samples were assigned to the proneural subtype, 6 samples were assigned to the mesenchymal subtype, and 3 samples were assigned to the neural subtype. The AOs with nodular and ringlike contrast enhancements were more frequently classified as mesenchymal than were AOs with blurry or no contrast enhancement (5/11 vs 1/14, $P=.05$).

Table 2. The MRI features of the 50 patients according to 1p/19q codeletion and IDH mutation

	Total, *n* (%)	1p/19q Codeletion, *n* (%)			*IDH* Mutation, *n* (%)		
		Yes	No	*P*	Yes	No	*P*
Topography							
Frontal	35 (70)	32 (82)	3 (27)	.001	33 (77)	2 (28)	.02
Temporal	8 (16)	5 (13)	3 (27)	NS	7 (16)	1 (14)	NS
Parietal	3 (6)	1 (2)	2 (18)	NS	1 (2)	2 (28)	.05
Occipital	3 (6)	1 (2)	2 (18)	NS	2 (5)	1 (14)	NS
Insula	18 (36)	13 (33)	5 (45)	NS	15 (35)	3 (43)	NS
Corpus callosum	15 (30)	13 (33)	2 (18)	NS	14 (32)	1 (14)	NS
Extension							
Unilobar	32 (64)	25 (64)	7 (64)	NS	28 (65)	4 (57)	NS
Multilobar	18 (36)	14 (36)	4 (36)	NS	15 (35)	3 (43)	NS
Contrast enhancement							
No	13 (26)	12 (31)	1 (10)	NS	12 (28)	1 (15)	NS
Yes	37 (74)	27 (69)	10 (90)	NS	31 (72)	6 (85)	NS
Blurry	9 (18)	9 (23)	0 (0)	NS	9 (21)	0 (0)	NS
Nodular	17 (34)	11 (28)	6 (54)	NS	15 (35)	2 (28)	NS
Ringlike	11 (22)	7 (18)	4 (36)	NS	7 (16)	4 (57)	.03
Tumoral borders							
Sharp	19 (38)	15 (39)	4 (36)	NS	17 (41)	2 (28)	NS
Indistinct	30 (62)	23 (60)	7 (63)	NS	25 (59)	5 (72)	NS
Intratumoral signal							
Heterogeneous T1	42 (84)	35 (89)	7 (63)	$P=.06$	33 (77)	5 (45)	NS
Heterogeneous T2 or FLAIR	37 (74)	33 (84)	4 (36)	$P=.003$	34 (79)	3 (43)	$P=.06$
Other							
Intratumoral cyst	14 (28)	13 (33)	1 (9)	NS	14 (32)	0 (0)	NS
Median volume (cm^3)	108	120	70	$P=.06$	111	100	NS

Discussion

This study demonstrates that AO molecular subtypes are associated with different radiological characteristics and that, as previously shown with glioblastomas,[10–13] correlating AO imaging and molecular features can be used to approach molecular alterations implicated in tumor growth.

The 1p/19q codeletion was previously shown to be associated with frontal lobe location, intratumoral signal heterogeneity, and blurred tumor borders.[5–9] Except for the tumor border characteristics, our study confirmed these findings. The *IDH* mutation was also associated with distinct radiological features, including a frontal lobe location and a lower rate of ringlike contrast enhancement. These findings are very similar to those reported in recent series of glioblastomas, in which the *IDH*-mutated tumors were predominantly frontal and had a lower rate of ringlike contrast enhancement.[10,12,13] As *IDH* mutation precedes 1p/19q codeletion, it is likely that the preferential frontal lobe location of the 1p/19q-codeleted AOs is explained by the fact that nearly all 1p/19q-codeleted AOs are *IDH* mutated.[4,21] The predominant frontal lobe location of the *IDH*-mutated gliomas may be explained by a preferentially tumorigenic effect of this mutation in specific forebrain neural progenitors.[13,22]

Although 1p/19q codeletion and *IDH* mutation were associated with distinct imaging characteristics, we were not able to identify a specific radiological pattern associated with these molecular characteristics. Importantly, the ringlike contrast enhancement (which was more frequent in *IDH* wild-type AOs) was also observed in nearly 20% of 1p/19q-codeleted and *IDH*-mutated AOs. Other MRI techniques might be more powerful for identifying features specifically associated with 1p/19q codeletion or *IDH* mutation. MRI texture analysis has been shown to predict 1p/19q codeletion with high sensitivity and specificity in low-grade gliomas,[23] and several studies have suggested that diffusion,[24] perfusion,[25–27] and MR spectroscopy[28] may also help to noninvasively identify 1p/19q codeletion. However, a recent study has demonstrated that the use of multimodal MRI only marginally improves the accuracy of conventional MRI for the identification of 1p/19q codeletion.[29] In contrast, MR spectroscopy seems to be a particularly promising technique for identifying *IDH*-mutated gliomas, as it can detect the intratumoral production of 2-hydroxyglutarate that specifically results from this mutation.[30,31]

In the 1p/19q-codeleted AOs, contrast enhancement was associated with a larger tumor volume and distinct histological, genomic, and gene expression features. Although all of the cases demonstrated endothelial hyperplasia, contrast enhancement was associated with microvascular proliferation, necrosis, and a higher proliferation index. At the genomic level, contrast enhancement was associated with chromosome 9p loss, *CDKN2A* loss, and chromosome instability. These findings are consistent with previous studies showing that chromosome 9p loss and *CDKN2A* loss are implicated in tumor progression[32] and the development of

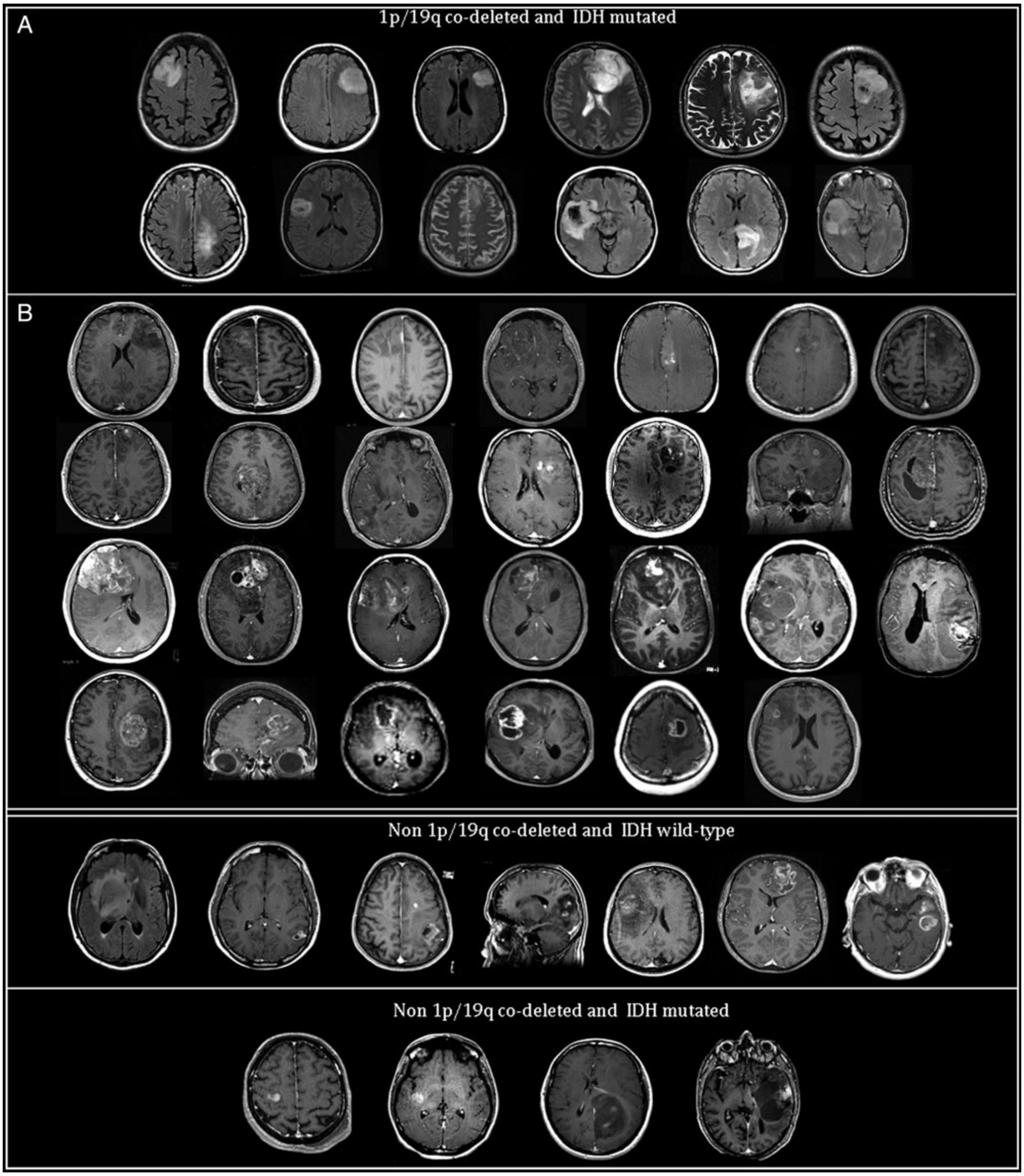

Fig. 2. Representative MRIs of the 50 patients classified according to their 1p/19q codeletion and *IDH* mutation status. The MRIs of 1p/19q-codeleted AOs were further classified according to contrast enhancement. Upper panel: 1p/19q-codeleted and IDH-mutated AOs without (A) and with contrast enhancement (B). Middle panel: AOs without 1p/19q codeletion and without *IDH* mutation. Lower panel: Non-1p/19q-codeleted AOs with *IDH* mutation.

microvascular proliferation in 1p/19q-codeleted oligodendrogliomas.[33] Both CDKN2A and p14ARF (the alternative *CDKN2A* gene product) have been shown to play anti-angiogenic roles.[34–39] Specifically, CDKN2A has been demonstrated to downregulate VEGF expression in gliomas[35] and to inhibit colon tumor angiogenesis.[40] The murine homolog of p14ARF, P19(ARF), has been shown to inhibit angiogenesis through the translational control of VEGFA mRNA.[34] At the gene expression level, contrast enhancement in 1p/19q-codeleted AOs was associated with the expression of angiogenesis-related genes; the expression of several of these genes, including VEGFA and ANGPT2, was positively correlated with tumor volume. Interestingly, most of the angiogenesis-related genes upregulated in the contrast-enhanced 1p/19q-codeleted AOs were previously shown to be upregulated in glioblastoma-associated vessels, suggesting that despite completely different genetic backgrounds, 1p/19q-codeleted AOs and glioblastomas have similar angiogenic profiles.[20] Therefore, anti-angiogenic therapies developed for glioblastomas may also be active in 1p/19q-codeleted AOs. Recent studies have demonstrated that targeting ANGPT2 could greatly enhance the efficacy

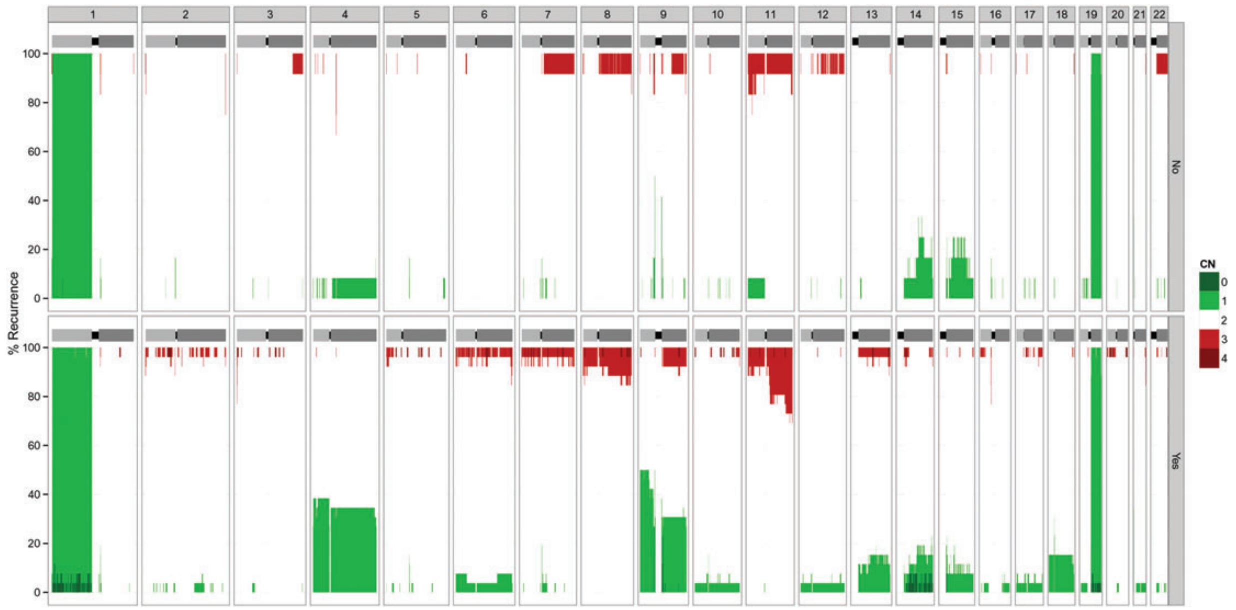

Fig. 3. Copy number alterations in 1p/19q-codeleted AOs. (Top) AO without contrast enhancement. (Bottom) AO with contrast enhancement. Genomic gain and genomic loss are indicated in red and green, respectively.

Table 3. List of the angiogenesis-related genes upregulated in contrast-enhanced ($n = 18$) vs non-contrast-enhanced ($n = 7$) 1p/19q-codeleted AOs (fold change ≥ 2, $P < .005$)

Gene Symbol	Fold Change	Gene Ontology	Upregulated in GBM-associated Blood Vessels	Role	Pearson Correlation Coefficient with tumor volume, r
COL1A1	11.3	Blood vessel development	Yes[42]		0.45 ($P = .03$)
COL3A1	8.1	Cell adhesion	Yes[20]		0.6 ($P = .002$)
COL1A2	4.6	Blood vessel development	Yes[20]		0.6 ($P = .003$)
ANGPT2	4.3	Angiogenesis	Yes[20]	Angiogenic[41]	0.57 ($P = .004$)
CD93	3.8	Cell adhesion	Yes[20]	Angiogenic[43]	0.41 ($P = .04$)
COL4A1	3.8	Angiogenesis	Yes[42]		0.47 ($P = .02$)
COL4A2	3.3	ECM organization	Yes[20]	Anti-angiogenic[44]	0.42 ($P = .04$)
TIMP1	3.2	ECM organization		Anti-angiogenic[45]	0.56 ($P = .004$)
COL6A3	3	Cell adhesion	Yes[20]		0.42 ($P = .04$)
HMOX1	2.7	Angiogenesis		Angiogenic[46]	NS
ENPEP	2.6	Angiogenesis	Yes[20]	Angiogenic[47]	NS
VEGFA	2.6	Angiogenesis		Angiogenic[48]	0.45 ($P = .02$)
NID2	2.4	Cell adhesion	Yes[20]		0.41 ($P = .04$)
ELTD1	2.4	Neuropeptide signaling	Yes[20]		NS
FN1	2.3	Cell adhesion	Yes[20]	Angiogenic[49]	NS
VWF	2.3	Blood coagulation		Anti-angiogenic[50]	0.44 ($P = .03$)
COL15A1	2.2	Angiogenesis		Anti-angiogenic[51]	NS
MYOF	2.2	VEGFR signaling pathway		Angiogenic[52]	NS
IGFBP4	2.1	Cell proliferation	Yes[20]	Anti-angiogenic[53]	NS
MYOIB	2.1	Regulation of cell shape	Yes[20]		NS
TFPI	2	Blood coagulation		Anti-angiogenic[54]	NS
SPRY1	2	EGFR signaling	Yes[20]	Anti-angiogenic[55]	NS

Abbreviations: GBM, glioblastoma multiforme; COL1A1, collagen, type I, alpha 1; COL3A1, collagen, type III, alpha 1; COL1A2, collagen, type I, alpha 2; CD93, CD93 molecule; COL4A1, collagen, type IV, alpha 1; COL4A2, collagen, type IV, alpha 2; ECM, extracellular matrix; TIMP1, tissue inhibitor of metalloproteinase 1; COL6A3, collagen, type VI, alpha 3; HMOX1, hemeoxygenase (decycling) 1; ENPEP, aminopeptidase A; NID2, nidogen 2; ELTD1, EGF, latrophilin and 7 transmembrane domain containing 1; FN1, fibronectin 1; VWF, von Willebrand factor; COL15A1, collagen, type XV, alpha 1; MYOF, myoferlin; IGFBP4, insulin-like growth factor binding protein 4; MYO1B, myosin 1B; TFPI, tissue factor pathway inhibitor; SPRY1, sprouty homolog 1, antagonist of fibroblast growth factor signaling (Drosophila).

of anti-VEGF treatments.[41] As ANGPT2 was the most overexpressed angiogenic gene in the contrast-enhanced 1p/19q-codeleted AOs, it might be a particularly interesting target in these tumors.

This study has several limitations. Besides its retrospective nature, it was based on the analysis of only conventional MRI characteristics. In addition, due to the prospective nature of the POLA network, the follow-up was too limited to perform correlations with the outcomes. Nevertheless, this study provides additional evidence of the relationship between AO imaging and molecular heterogeneity and shows that correlating pathological, radiological, and molecular data is an interesting strategy for identifying molecular alterations associated with tumor progression.

Supplementary Material

Supplementary material is available at *Neuro-Oncology Journal* online (http://neuro-oncology.oxfordjournals.org/).

Funding

This work was funded by the French Institut National du Cancer and part of the national program Cartes d'Identité des Tumeurs (http://cit.ligue-cancer.net/), funded and developed by the Ligue Nationale Contre le Cancer.

Acknowledgment

Genomic data mining was done in collaboration with Simon de Bernard and Altrabio.

Conflict of interest statement. The authors have no conflict of interest to declare. The funding sources had no role in study design, data collection and analysis, decision to publish, or preparation of the manuscript.

References

1. Ricard D, Idbaih A, Ducray F, Lahutte M, Hoang-Xuan K, Delattre JY. Primary brain tumours in adults. *Lancet*. 2012;379:1984–1996.
2. Cairncross G, Wang M, Shaw E, et al. Phase III trial of chemoradiotherapy for anaplastic oligodendroglioma: long-term results of RTOG 9402. *J Clin Oncol*. 2013;31:337–343.
3. van den Bent MJ, Brandes AA, Taphoorn MJ, et al. Adjuvant procarbazine, lomustine, and vincristine chemotherapy in newly diagnosed anaplastic oligodendroglioma: long-term follow-up of EORTC brain tumor group study 26951. *J Clin Oncol*. 2013;31:344–350.
4. Labussiere M, Idbaih A, Wang XW, et al. All the 1p19q codeleted gliomas are mutated on IDH1 or IDH2. *Neurology*. 2010;74(23): 1886–1890.
5. Jenkinson MD, du Plessis DG, Smith TS, Joyce KA, Warnke PC, Walker C. Histological growth patterns and genotype in oligodendroglial tumours: correlation with MRI features. *Brain*. 2006;129:1884–1891.
6. Kim JW, Park CK, Park SH, et al. Relationship between radiological characteristics and combined 1p and 19q deletion in World Health Organization grade III oligodendroglial tumours. *J Neurol Neurosurg Psychiatry*. 2011;82:224–227.
7. Laigle-Donadey F, Martin-Duverneuil N, Lejeune J, et al. Correlations between molecular profile and radiologic pattern in oligodendroglial tumors. *Neurology*. 2004;63:2360–2362.
8. Megyesi JF, Kachur E, Lee DH, et al. Imaging correlates of molecular signatures in oligodendrogliomas. *Clin Cancer Res*. 2004;10: 4303–4306.
9. Zlatescu MC, TehraniYazdi A, Sasaki H, et al. Tumor location and growth pattern correlate with genetic signature in oligodendroglial neoplasms. *Cancer Res*. 2001;61:6713–6715.
10. Carrillo JA, Lai A, Nghiemphu PL, et al. Relationship between tumor enhancement, edema, IDH1 mutational status, MGMT promoter methylation, and survival in glioblastoma. *AJNR Am J Neuroradiol*. 2012;33:1349–1355.
11. Diehn M, Nardini C, Wang DS, et al. Identification of noninvasive imaging surrogates for brain tumor gene-expression modules. *Proc Natl Acad Sci U S A*. 2008;105:5213–5218.
12. Ellingson BM, Lai A, Harris RJ, et al. Probabilistic radiographic atlas of glioblastoma phenotypes. *AJNR Am J Neuroradiol*. 2013;34:533–540.
13. Lai A, Kharbanda S, Pope WB, et al. Evidence for sequenced molecular evolution of IDH1 mutant glioblastoma from a distinct cell of origin. *J Clin Oncol*. 2011;29:4482–4490.
14. Idbaih A, Ducray F, Dehais C, et al. SNP array analysis reveals novel genomic abnormalities including copy neutral loss of heterozygosity in anaplastic oligodendrogliomas. *PLoS One*. 2012;7:e45950.
15. Louis DN, Ohgaki H, Wiestler OD, et al. The 2007 WHO classification of tumours of the central nervous system. *Acta Neuropathol*. 2007;114: 97–109.
16. Ducray F, de Reynies A, Chinot O, et al. An ANOCEF genomic and transcriptomic microarray study of the response to radiotherapy or to alkylating first-line chemotherapy in glioblastoma patients. *Mol Cancer*. 2010;9:234.
17. Sanson M, Marie Y, Paris S, et al. Isocitrate dehydrogenase 1 codon 132 mutation is an important prognostic biomarker in gliomas. *J Clin Oncol*. 2009;27:4150–4154.
18. Verhaak RG, Hoadley KA, Purdom E, et al. Integrated genomic analysis identifies clinically relevant subtypes of glioblastoma characterized by abnormalities in PDGFRA, IDH1, EGFR, and NF1. *Cancer Cell*. 2010;17: 98–110.
19. Subramanian A, Tamayo P, Mootha VK, et al. Gene set enrichment analysis: a knowledge-based approach for interpreting genome-wide expression profiles. *Proc Natl Acad Sci U S A*. 2005;102:15545–15550.
20. Dieterich LC, Mellberg S, Langenkamp E, et al. Transcriptional profiling of human glioblastoma vessels indicates a key role of VEGF-A and TGFbeta2 in vascular abnormalization. *J Pathol*. 2012;228:378–390.
21. Watanabe T, Nobusawa S, Kleihues P, Ohgaki H. IDH1 mutations are early events in the development of astrocytomas and oligodendrogliomas. *Am J Pathol*. 2009;174:1149–1153.
22. Persson AI, Petritsch C, Swartling FJ, et al. Non-stem cell origin for oligodendroglioma. *Cancer Cell*. 2010;18:669–682.
23. Brown R, Zlatescu M, Sijben A, et al. The use of magnetic resonance imaging to noninvasively detect genetic signatures in oligodendroglioma. *Clin Cancer Res*. 2008;14:2357–2362.
24. Jenkinson MD, Smith TS, Brodbelt AR, Joyce KA, Warnke PC, Walker C. Apparent diffusion coefficients in oligodendroglial tumors characterized by genotype. *J Magn Reson Imaging*. 2007;26: 1405–1412.
25. Law M, Brodsky JE, Babb J, et al. High cerebral blood volume in human gliomas predicts deletion of chromosome 1p: preliminary results of molecular studies in gliomas with elevated perfusion. *J Magn Reson Imaging*. 2007;25:1113–1119.
26. Whitmore RG, Krejza J, Kapoor GS, et al. Prediction of oligodendroglial tumor subtype and grade using perfusion weighted magnetic resonance imaging. *J Neurosurg*. 2007;107:600–609.

27. Narang J, Jain R, Scarpace L, et al. Tumor vascular leakiness and blood volume estimates in oligodendrogliomas using perfusion CT: an analysis of perfusion parameters helping further characterize genetic subtypes as well as differentiate from astroglial tumors. *J Neurooncol*. 2011;102:287–293.
28. Chawla S, Krejza J, Vossough A, et al. Differentiation between oligodendroglioma genotypes using dynamic susceptibility contrast perfusion-weighted imaging and proton MR spectroscopy. *AJNR Am J Neuroradiol*. 2013;34:1542–1549.
29. Fellah S, Caudal D, De Paula AM, et al. Multimodal MR imaging (diffusion, perfusion, and spectroscopy): is it possible to distinguish oligodendroglial tumor grade and 1p/19q codeletion in the pretherapeutic diagnosis? *AJNR Am J Neuroradiol*. 2013;34: 1326–1333.
30. Choi C, Ganji SK, DeBerardinis RJ, et al. 2-Hydroxyglutarate detection by magnetic resonance spectroscopy in IDH-mutated patients with gliomas. *Nat Med*. 2012;18:624–629.
31. Elkhaled A, Jalbert LE, Phillips JJ, et al. Magnetic resonance of 2-hydroxyglutarate in IDH1-mutated low-grade gliomas. *Sci Transl Med*. 2012;4:116ra115.
32. Bigner SH, Rasheed BK, Wiltshire R, McLendon RE. Morphologic and molecular genetic aspects of oligodendroglial neoplasms. *Neuro Oncol*. 1999;1:52–60.
33. Godfraind C, Rousseau E, Ruchoux MM, Scaravilli F, Vikkula M. Tumour necrosis and microvascular proliferation are associated with 9p deletion and CDKN2A alterations in 1p/19q-deleted oligodendrogliomas. *Neuropathol Appl Neurobiol*. 2003;29:462–471.
34. Kawagishi H, Nakamura H, Maruyama M, et al. ARF suppresses tumor angiogenesis through translational control of VEGFA mRNA. *Cancer Res*. 2010;70:4749–4758.
35. Harada H, Nakagawa K, Iwata S, et al. Restoration of wild-type p16 down-regulates vascular endothelial growth factor expression and inhibits angiogenesis in human gliomas. *Cancer Res*. 1999;59: 3783–3789.
36. McKeller RN, Fowler JL, Cunningham JJ, et al. The Arf tumor suppressor gene promotes hyaloid vascular regression during mouse eye development. *Proc Natl Acad Sci U S A*. 2002;99:3848–3853.
37. Alhaja E, Adan J, Pagan R, et al. Anti-migratory and anti-angiogenic effect of p16: a novel localization at membrane ruffles and lamellipodia in endothelial cells. *Angiogenesis*. 2004;7:323–333.
38. Zhang J, Lu A, Li L, Yue J, Lu Y. P16 modulates VEGF expression via its interaction with HIF-1alpha in breast cancer cells. *Cancer Invest*. 2010;28:588–597.
39. Takeuchi H, Ozawa S, Shih CH, et al. Loss of p16INK4a expression is associated with vascular endothelial growth factor expression in squamous cell carcinoma of the esophagus. *Int J Cancer*. 2004;109: 483–490.
40. Gibson SL, Dai CY, Lee HW, et al. Inhibition of colon tumor progression and angiogenesis by the Ink4a/Arf locus. *Cancer Res*. 2003;63: 742–746.
41. Gerald D, Chintharlapalli S, Augustin HG, Benjamin LE. Angiopoietin-2: an attractive target for improved antiangiogenic tumor therapy. *Cancer Res*. 2013;73:1649–1657.
42. Liu Y, Carson-Walter EB, Cooper A, Winans BN, Johnson MD, Walter KA. Vascular gene expression patterns are conserved in primary and metastatic brain tumors. *J Neurooncol*. 2010;99:13–24.
43. Kao YC, Jiang SJ, Pan WA, et al. The epidermal growth factor-like domain of CD93 is a potent angiogenic factor. *PLoS One*. 2012;7: e51647.
44. Hwang-Bo J, Yoo KH, Park JH, Jeong HS, Chung IS. Recombinant canstatin inhibits angiopoietin-1-induced angiogenesis and lymphangiogenesis. *Int J Cancer*. 2012;131:298–309.
45. Reed MJ, Koike T, Sadoun E, Sage EH, Puolakkainen P. Inhibition of TIMP1 enhances angiogenesis in vivo and cell migration in vitro. *Microvasc Res*. 2003;65:9–17.
46. Zhang W, Zhang X, Lu H, Matsukura M, Zhao J, Shinohara M. Silencing heme oxygenase-1 gene expression in retinal pigment epithelial cells inhibits proliferation, migration and tube formation of cocultured endothelial cells. *Biochem Biophys Res Commun*. 2013;434:492–497.
47. Marchio S, Lahdenranta J, Schlingemann RO, et al. Aminopeptidase A is a functional target in angiogenic blood vessels. *Cancer Cell*. 2004;5: 151–162.
48. Idbaih A, Ducray F, Sierra Del Rio M, Hoang-Xuan K, Delattre JY. Therapeutic application of noncytotoxic molecular targeted therapy in gliomas: growth factor receptors and angiogenesis inhibitors. *Oncologist*. 2008;13:978–992.
49. Newman AC, Chou W, Welch-Reardon KM, et al. Analysis of stromal cell secretomes reveals a critical role for stromal cell-derived hepatocyte growth factor and fibronectin in angiogenesis. *Arterioscler Thromb Vasc Biol*. 2013;33:513–522.
50. Franchini M, Frattini F, Crestani S, Bonfanti C, Lippi G. von Willebrand factor and cancer: a renewed interest. *Thromb Res*. 2013;131: 290–292.
51. Sasaki T, Larsson H, Tisi D, Claesson-Welsh L, Hohenester E, Timpl R. Endostatins derived from collagens XV and XVIII differ in structural and binding properties, tissue distribution and anti-angiogenic activity. *J Mol Biol*. 2000;301:1179–1190.
52. Bernatchez PN, Acevedo L, Fernandez-Hernando C, et al. Myoferlin regulates vascular endothelial growth factor receptor-2 stability and function. *J Biol Chem*. 2007;282:30745–30753.
53. Moreno MJ, Ball M, Rukhlova M, et al. IGFBP-4 Anti-Angiogenic and Anti-Tumorigenic Effects Are Associated with Anti-Cathepsin B *Activity*. *Neoplasia*. 2013;15:554–567.
54. Holroyd EW, White TA, Pan S, Simari RD. Tissue factor pathway inhibitor as a multifunctional mediator of vascular structure. *Front Biosci (Elite Ed)*. 2012;4:392–400.
55. Sabatel C, Cornet AM, Tabruyn SP, et al. Sprouty1, a new target of the angiostatic agent 16K prolactin, negatively regulates angiogenesis. *Mol Cancer*. 2010;9:231.